JOURNAL OF APPLIED ELECTROCHEMISTRY 3 (1973) 241–242

The electrochemical behaviour of cobalt in alkaline nitrate melts at different temperatures

J. J. PODESTÁ, R. C. V. PIATTI AND A. J. ARVÍA

Instituto de Investigaciones Fisicoquímicas Teóricas y Aplicadas, Universidad Nacional de La Plata, Argentina

Received 12 February 1973

The electrochemical behaviour of cobalt in molten alkali nitrates in the temperature range from 141 to 321°C has been investigated. At lower temperatures the metal dissolves as Co(II); the oxidation product at higher temperatures is Co_3O_4. Nitrogen oxides are also formed. Passivation and localized corrosion occur under definite anode potential, Co(II) concentration and temperature conditions. These effects have been studied by non-stationary measurements. Co(II) dissolved in the melt can be electrodeposited either on cobalt or platinum cathodes.

1. Introduction

The electrochemical behaviour of iron and nickel in molten alkali nitrates has been reported previously, [1, 2]. The main purpose of these studies was to determine the potential regions related to immunity, corrosion and passivity of these metals, as theoretically established through the thermodynamic potential/pO^{2-} diagrams, [3, 4] and also to obtain information on the kinetics of those processes.

Both the kinetics as well as the types of metallic oxides involved in the electrochemical oxidation of iron and nickel are different. This led us to extend the systematic study to cobalt electrodes dipped in molten alkali nitrates in order to obtain information attempting to establish a regular transition of the electrochemical characteristics within this group of metals to see whether there is any correlation with atomic configuration.

2. Experimental

The experimental technique employed in this study was the same as described previously [1, 2]. Cobalt wires (J. Matthey 99·997%, 0·5 mm diameter) were used as electrodes. Runs were also made with cold rolled cobalt plates (J. Matthey 99·995%, apparent area between 1 and 6 cm^2).

The electrolyte was a KNO_3-$NaNO_3$-$LiNO_3$ melt having the eutectic composition (44·5-37·5-18 mole %, respectively) in the temperature range from 141 to 321°C.

The counter electrode was a platinum plate of large area (*c.* 10 cm^2) and the reference electrode was a platinum electrode dipped into the alkali nitrate melt. This electrode gives an arbitrary but otherwise reproducible reference potential [1, 2].

3. Results

3.1. *Products from the anodic reaction*

When a cobalt electrode is anodized at 3–4 mA cm^{-2} in the melt at 250°C, gases containing nitrogen oxides, principally NO_2 and N_2O, are formed while the melt/electrode interphase acquires a violet tinge which is characteristic of Co(II) dissolved in the molten nitrate [5, 6],

and the metal becomes covered with a Co_3O_4 film. The oxide was identified by X-ray diffractograms, which exhibited only the α-Co and Co_3O_4 characteristic peaks. The same oxide film was found after immersion of the metal in the melt at 250°C for 10 h.

When the anodic dissolution proceeds at low c.d. and at temperatures below 260°C or thereabouts, dissolved Co(II) remains as a stable solute in the melt. At higher temperatures the formation of a soluble species was also observed, but the latter decomposed to yield Co_3O_4.

The electrolysis carried out at 350°C yielded the same gases and oxide formation on the metal but instead of giving soluble Co(II), black Co_3O_4 was precipitated in the melt. The latter was identified by chemical and physical methods (X-ray diffraction and electron microscopy).

At 250°C and at 276°C, the amount of metal dissolved per unit charge passed at $i = 1{\cdot}0$ mA cm^{-2} corresponded to 2·66 (±5%) unit charge per metal atom, in good agreement with the composition of Co_3O_4.

Localized corrosion is observed in the temperature range 141–168°C. Apparently the pitting effect is less marked at about 215°C and the metal corrosion becomes more uniform.

3.2. *Stationary current/potential curves*

After immersion in the melt, the initial potential of cobalt lies at −0·7 V or thereabouts. This potential is unstable, changing in a few minutes to more positive values. The rate of this change depends on the temperature and the Co(II) ion concentration in the melt. The higher the temperature the more positive the initial potential.

The potentiostatic E/I curves, involving current readings at infinite time, depend at least on (i) the temperature; (ii) the Co(II) ion concentration in the melt and (iii) the direction of the potential change.

At 141°C the semi-logarithmic plots of E/I curves of two runs (Fig. 1a) exhibit three different regions identified in the drawing as A, B and C. Region A extends from the immersion potential over a range of 0·15–0·20 V and corresponds to a nonlinear E/log i relationship.

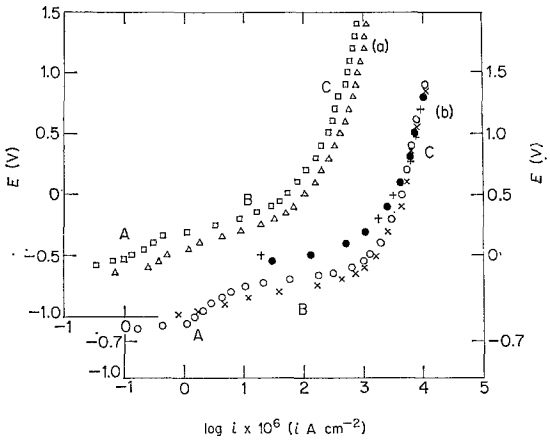

Fig. 1. Semilogarithmic plots of anodic potentiostatic E/i curves. a, Runs at 141°C (□,△) Co(II) in the melt initially absent, E changed upwards; b, Runs at 168°C (○,×), Co(II) in the melt initially absent, E changed upwards; (●,+) Co(II) in the melt, E changed downwards.

Region B exhibits a linear E/log i plot with a slope close to $2{\cdot}3(2RT/F)$ over nearly two logarithmic decades of current density, covering about 0·30 V. Finally, region C presents a rapid increase of electrode polarization. No linear E/log i relationship is observed in this region. In the returning E/I curve (Fig. 1b), regions A and B are absent. In this case, as well as in the case of electrolysis interruption at high anodic potentials, the rest potential, E_r, attained by the cobalt electrode, is stable and located 0·45 V more positive than the initial immersion potential.

When Co(II) is present in the melt, region A exhibits a passivation effect, as soon as the applied potential exceeds 0·05 V above the immersion potential (Fig. 1b). At 168°C the apparent Tafel region has a slope which has about half the value reported at lower temperatures. The rest of the E/I curve coincides with the one already described. However, if a second E/I curve is run, starting from the rest potential upwards, region C is the only one recorded. Now, the shape of the E/I curve is independent of the presence of Co(II) ion in the melt.

The shapes of regions A and B continue changing when temperature increases, this is noticed particularly in the continuous decrease of the apparent Tafel slope with temperature (Fig. 2a). At 215°C, for instance, (Fig. 2b), a passivity potential is observed at −0·43 V and at more positive potentials, the E/I curve exhibits two

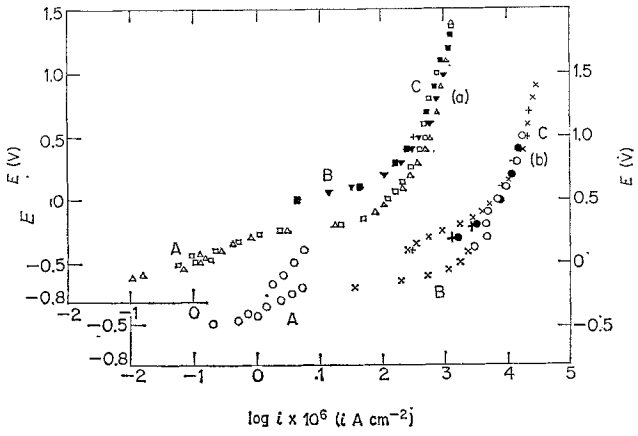

Fig. 2. Semilogarithmic plots of anodic potentiostatic E/i curves. a Runs at 183°C (□,△) Co(II) in the melt initially absent, E changed upwards; (▼,■) with Co(II) in the melt, E changed downwards; b Runs at 215°C(○,×) Co(II) in the melt initially absent, E changed upwards; (●,+) with Co(II) in the melt, E changed downwards.

breaks, one at −0·2 V and another at 0·1 V. The latter is close to the rest potential attained after electrolysis interruption at high anodic potentials.

At this temperature there is no linear E/log i region when the polarization curve is run from the immersion potential upwards. The returning curve behaves similarly to the one already described at lower temperatures.

At 235°C, region A is not found and the immersion potential is found at −0·22 V. The E/I curve presents a break at the rest potential, the latter at higher temperatures becoming more positive (Fig. 3a). However, the difference between the rest potential and the immersion potential is, as before, equal to 0·40–0·47 V. In spite of the changes in the E/I curves just described, this potential difference is nearly unchanged within the whole temperature range.

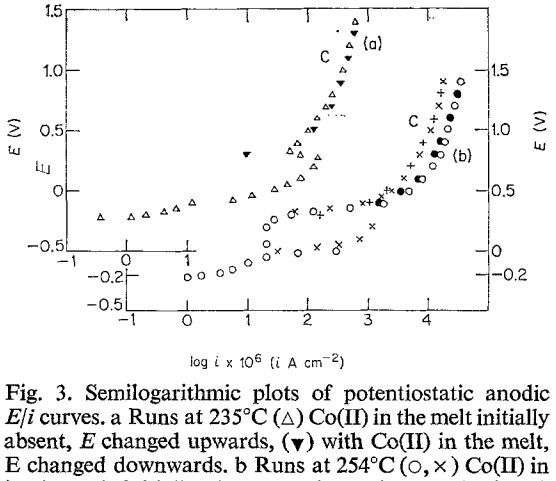

Fig. 3. Semilogarithmic plots of potentiostatic anodic E/i curves. a Runs at 235°C (△) Co(II) in the melt initially absent, E changed upwards, (▼) with Co(II) in the melt, E changed downwards. b Runs at 254°C (○,×) Co(II) in in the melt initially absent, E changed upwards, (●,+) with Co(II) in the melt, E changed downwards.

At 254°C, in the absence of Co(II), the immersion potential lies at about −0·2 V, and passivity is observed from about 0 V (Fig. 3b) up to 0·25 V when a residual limiting current is found. At higher anodic potentials, only region C is observed. In the presence of Co(II) the E/I curve starts from a potential, which in the absence of Co(II) corresponds to the passivity onset. At higher anodic potentials the features of the E/I curves are the same as already described.

At 320°C the initial potential is −0·25 V, the passivity onset occurs at −0·15 V and the rest potential lies at 0·40 V.

3.3. *Potentiostatic current/time response at the discontinuity of the E/I curve*

Figs. 4 and 5 show records of the periodic current fluctuations at constant potential. At 250°C for a melt containing Co(II) ions this response first appears at 0·05 V above the immersion potential, the average current being *c.* 35 μA. Each period shows an abrupt anodic current increase up to *c.* 60 μA, then a decrease

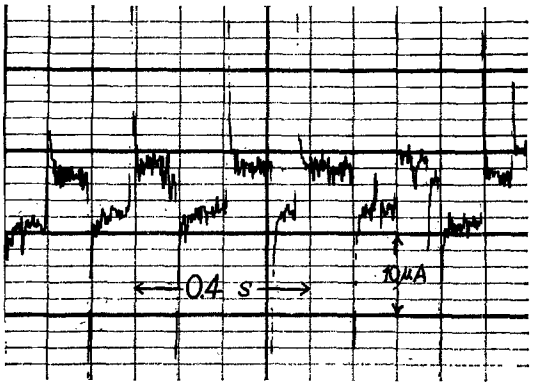

Fig. 4. Potentiostatic I/t response at the discontinuity of the E/i curve, 250°C, E = 0·05 V above the immersion potential.

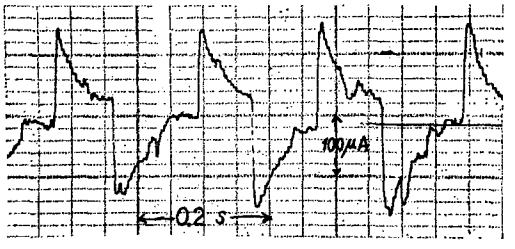

Fig. 5. Potentiostatic I/t response at the discontinuity of the E/i curve, 250°C, E = 0·35 V above the immersion potential.

to the average current value and finally a rather abrupt fall down to about 15 μA. The characteristic period of this effect is 0·4 Hz.

At about 0·350 V above the immersion potential where a net discontinuity in the E/I curve exists, the current fluctuates around an average value of *c.* 200 μA. Each period comprises an initial anodic current jump up to *c.* 350 μA, then a decrease down to its average value and finally a fall to *c.* 60 μA. The effect repeats at 0·2 Hz.

For any of the periodic effects just described, each cycle can be divided with respect to the average current, into a positive and a negative half-cycle.

The charge per cycle involved for the periodic effect recorded at the higher anodic potential is on the average 0·167 mC cm^{-2}. The charges involved at both half-cycles are 0·0275 mC cm^{-2} for the positive and 0·0260 mC cm^{-2} for the negative one. Therefore, an average number of $6{\cdot}14 \times 10^{13}$ Co atom cm^{-2} participates in each half-cycle. If the number of Co atoms per square centimetre is taken as $5{\cdot}9 \times 10^{15}$, then the electrode area participating in the electrode process is $1{\cdot}04 \times 10^{-2}$ times the total electrode area. This means that the actual current density associated with this phenomenon is *c.* 3·3 mA cm^{-2}.

The charges involved in the periodic current effect are much less than those corresponding to the formation of a film of homogeneous thickness on the metal surface. In spite of the 'noise' characterizing the periodic effect, it is possible to draw an average smooth I/t record to determine the corresponding average I/t dependence. Thus, during the positive half-cycle recorded at 0·350 V, the anodic current increases linearly with $t^{\frac{1}{2}}$. During the negative half-cycle it decreases linearly also with $t^{\frac{1}{2}}$.

The absolute slopes of both linear plots are very close. Thus, for the dissolution process $\Delta I/\Delta t^{\frac{1}{2}} = 0{\cdot}108$ mA $s^{-\frac{1}{2}}$ and for the passivation process $(\Delta I/\Delta t^{\frac{1}{2}}) = -0{\cdot}126$ mA $s^{-\frac{1}{2}}$. Unfortunately a similar analysis with the periodic effect recorded at lower potential with the present results is uncertain because of the high percentage of background noise.

3.4. *Current/time response to potentiostatic steps*

The I/t response to potentiostatic steps depends strongly on the magnitude of the potential step (rise-time 10^{-4} s). Fig. 6 shows the I/t response,

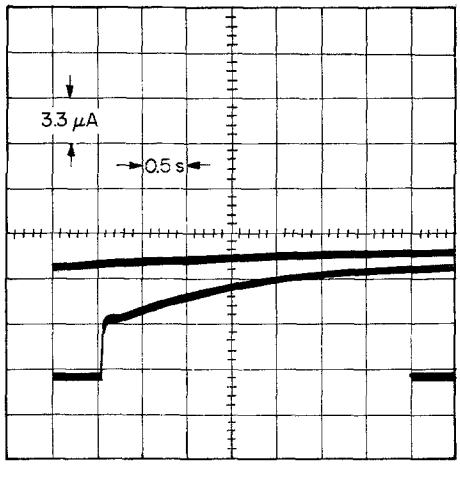

Fig. 6. I/t response to a potentiostatic step, 210°C. Immersion potential: −0·250 V; final potential: 0·100 V. Fresh electrode surface.

for a clean cobalt electrode whose immersion potential was −0·250 V, when a 0·350 V potentiostatic step is applied. There is an instantaneous current jump of about 4 μA, the current stabilizes for a short time and then it starts to rise to a value of the order of 10 μA.

Fig. 7 shows a recording starting from −0·120 V when a potential step of 0·170 V is applied. Within the first 0·1 s the I/t curve reaches a maximum and afterwards the current decreases down to a few μA.

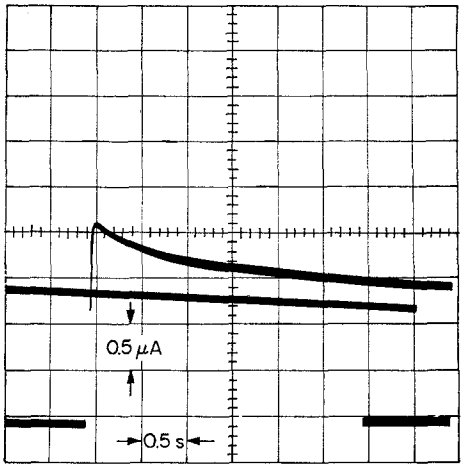

Fig. 7. I/t response to a potentiostatic step, 210°C. Immersion potential: −0·120 V; final potential: 0·050 V. Fresh electrode surface.

When the experiments are conducted with a previously anodized and partially cleaned cobalt electrode, the initial potential is about 0·09 V and when a potential step of 0·080 V is applied (Fig. 8), a region of rather constant current, of the order of 30 μA, is initially attained. After one second or thereabouts, the current decays with a particular 'noise' which apparently characterizes the onset of the passive state of the metal.

Additional differences are observed when anodized electrodes are used starting from 0·05 to 0·15 V. For small potential steps the response is coincident with that shown in Fig. 8, but for large anodic potentials two different responses are found. The first one (Fig. 9) shows initially,

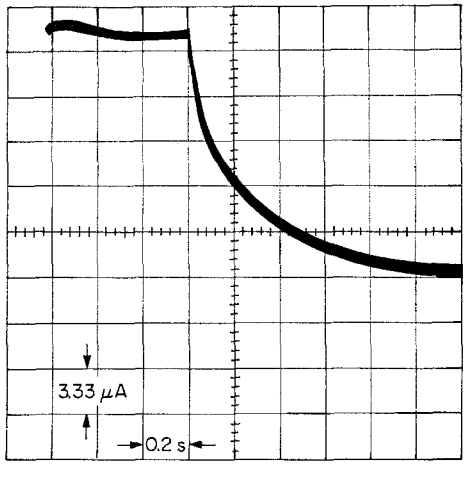

Fig. 8. I/t response to a potentiostatic step, 210°C. Immersion potential: 0·090 V; final potential: 0·170 V. Electrode previously used and partially cleaned.

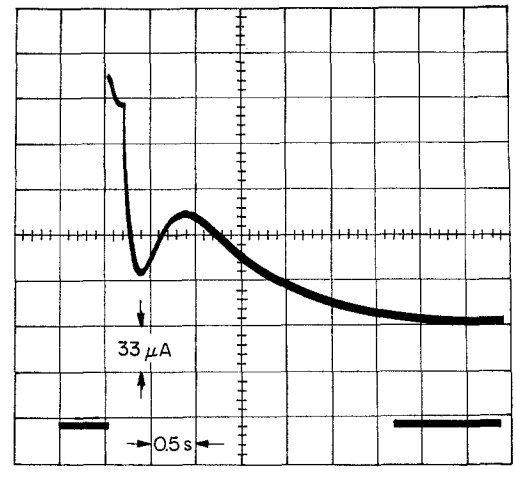

Fig. 9. I/t response to a potentiostatic step, 210°C. Immersion potential: 0·090 V; final potential: 0·280 V. Electrode previously used and partially cleaned.

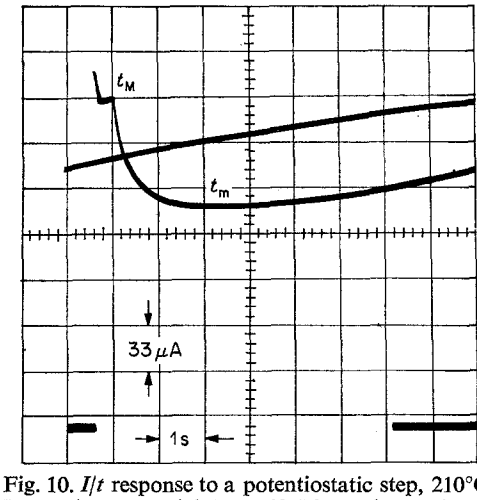

Fig. 10. I/t response to a potentiostatic step, 210°C. Immersion potential 0·090 V. Electrode previously anodized and partially cleaned.

the charging of the electrical double layer; at longer times, a maximum current is reached. The second type of behaviour (Fig. 10) corresponds to the existence of an initial current plateau; then the current decays down to a minimum value and finally it increases steadily up to its stationary value. Although both responses could be reproduced, the conditions for a standardized electrode surface could not be clearly established. Consequently no reliable quantitative relationship can be derived from the present results.

The I/t curves which exhibit a current maximum, without considering the double layer charging process, approach at different time scales, three limiting equations. At $t \rightarrow 0$, a linear I/t relationship is attained. Immediately after reaching the maximum, the current decay follows a linear function with $t^{\frac{1}{2}}$. Finally, at times exceeding that corresponding to the minimum current, the latter increases again near linearly with t, although at a rate which is much slower than that found at $t \rightarrow 0$. These current transients are therefore characterized by two definite times, t_M and t_m, which are respectively associated with the maximum and minimum currents. The initial part of these curves including the current maximum, can be described to a large extent by the following equation:

$$i = k\, t \exp\left[(t/2t_M)^2\right] \qquad (1)$$

where k is the charge transferred during the potentiostatic transient.

3.5. *The galvanostatic build-up of the anodic potential and its decay at current interruption*

Most of these experiments were made with electrodes at potentials close to the rest potential. The E/t curves can be separated into three different groups. When the current step is about 6 μA cm^{-2}, a steady potential increase occurs (Fig. 11). When anodic current pulses of the order of a few mA are applied to recently polished cobalt electrodes, the potential build-up exhibits a transition time which is related to the passivity onset (Fig. 12). If the same experiments

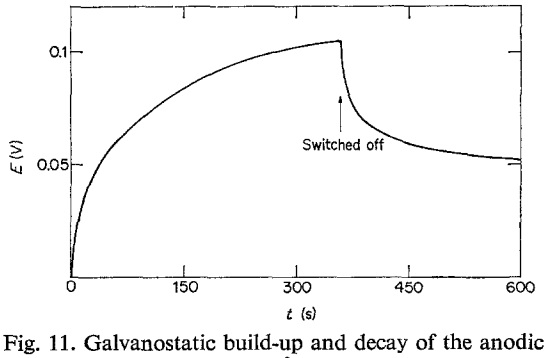

Fig. 11. Galvanostatic build-up and decay of the anodic potential, 210°C, i: 6 μAcm^{-2}.

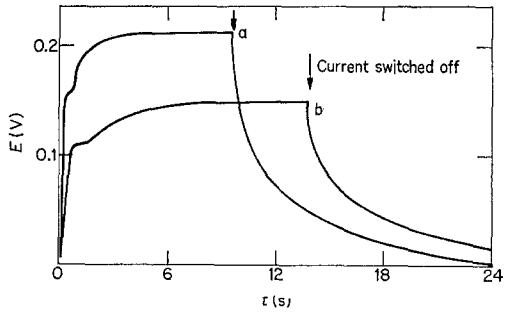

Fig. 12. Galvanostatic build-up and decay of the anodic potential, 210°C, (a) i = 12·7 mA cm^{-2}; (b) i = 4·2 mA cm^{-2}; fresh polished electrode.

are carried on with electrodes previously anodized at potentials corresponding to region C of the $E/\log I$ curve, a potential maximum is attained at a certain time; afterwards the potential decreases and approaches its steady value (Fig. 13). When an anodic current flowing

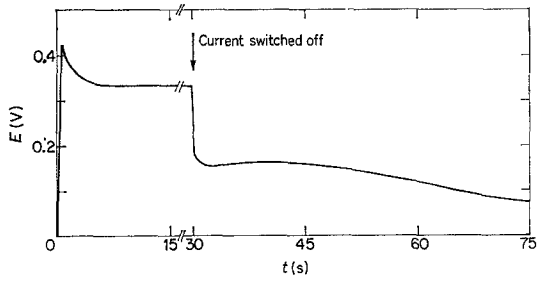

Fig. 13. Galvanostatic build-up and decay of the anodic potential, 210°C, i = 4·5 mA cm^{-2}. Previously anodized electrode.

through fresh electrodes is switched off (Figs. 11 and 12), the potential decays semi-logarithmically with time; the slope of the $E/\log t$ plot is of the order of 0·10 V per decade. The potential decay at electrodes previously anodized at high potentials is more complex than that corresponding to fresh electrodes. After a few seconds of current interruption a potential minimum is reached. Then the potential increases slightly

and finally, after 15 s or thereabouts, it decays regularly to attain the rest potential (Fig. 13).

When electrolysis proceeds with a cobalt anode, a localized corrosion is observed on its surface. This effect was clearly observed in the temperature region from 141 to 215°C.

3.6. *Cobalt electrodeposition*

The electrodeposition of cobalt from melts containing different Co(II) ion concentrations was attempted at 245°C. Besides yielding information about the cathodic reaction, these experiments should also yield data on a possible effect of the concentration of Co(II) ion on the rest potential and allow a coulometric relationship to be established between the dissolution and deposition processes. The different amounts of Co(II) ion in the melt were obtained from anodic dissolution of a cobalt electrode at potentials in the B region of the polarization curve.

To determine the influence of Co(II) ion on the rest potential, concentration cells involving two cobalt electrodes dipped in nitrate melts with different Co(II) ion concentration were made. The liquid junction potential of the concentration cell was neglected because of the ionic composition of the system. At 245°C and within the concentration range investigated, an apparent Nernstian relationship was found. However, due to the change of potential with time no definite conclusions can be derived from these results.

The cathodic E/I curves related to cobalt electrodeposition on platinum plate electrodes under different experimental conditions are shown in Fig. 14. They exhibit a starting potential which depends on the time elapsed since initiation of the electrolysis, but there is a cathodic limiting current within a potential range of *c.* 0·4 V. At constant composition and temperature, the cathodic limiting current obtained with static electrodes increases near linearly with Co(II) ion concentration, as determined coulometrically. It also increases by a factor of about 10 when the electrode vibrates.

The cathodic E/I curves can be linearized by plotting the applied potential against the log $[I_L/(I_L-I_C)]$, where I_L is the cathodic limiting current and I_C, the cathodic current read at the applied potential E (Fig. 15). The slope of the best straight line is close to 2·3 RT/F.

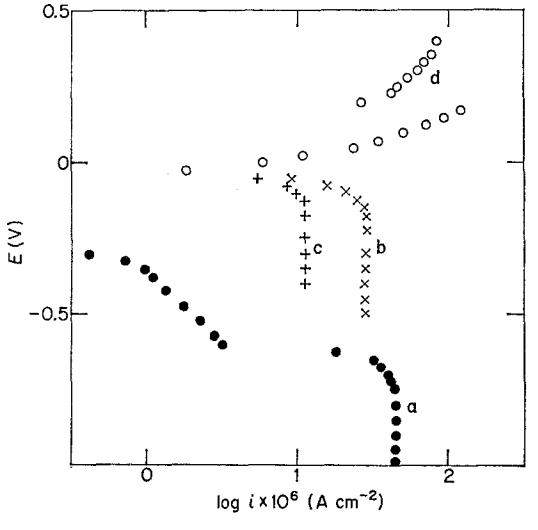

Fig. 14. Semilogarithmic plots of potentiostatic E/i curves at 245°C. a, Cathodic cobalt electrodeposition on platinum, Co(II): $2{\cdot}9\times10^{-4}$ mol kg^{-1}. b, Cathodic cobalt electrodeposition on an electrodeposited cobalt surface, Co(II): $1{\cdot}7\times10^{-3}$ mol kg^{-1}. c, Cathodic cobalt electrodeposition on an electrodeposited cobalt surface, Co(II): $0{\cdot}78\times10^{-3}$ mol kg^{-1}. Anodic cobalt dissolution from electrodeposited cobalt.

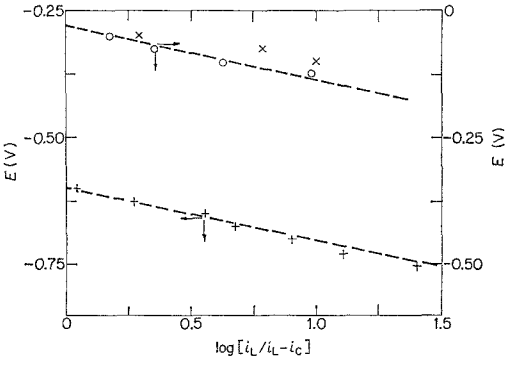

Fig. 15. $E/\log\,[i_L/(i_L-i_C)]$ plots for the cathodic cobalt electrodeposition. Data taken from Fig. 14. from (+) run a, (×) from run b and (○) from run c.

The correspondence between the amount of metal dissolved and the value of the cathodic limiting current may be altered by the partial precipitation of Co(II) as insoluble Co_3O_4.

4. Discussion

The E/I curves recorded for the cobalt/alkali

nitrate melt are rather complex. To interpret them, let us consider a temperature where Co(II) ionic species are stable in the melt. According to the equilibrium potential/pO^{2-} diagram for this system (Fig. 16), at pO^{2-} beyond 27,

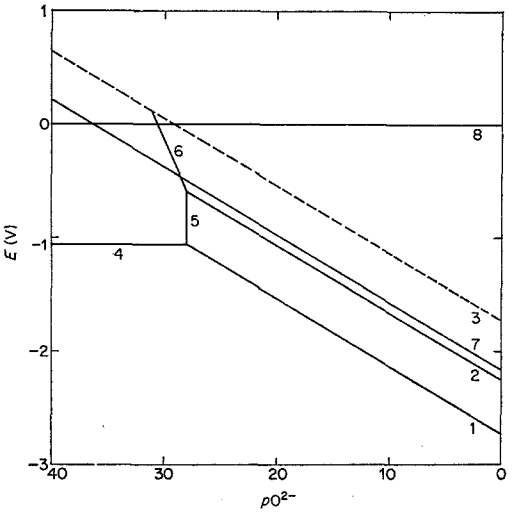

Fig. 16. Equilibrium potential/pO^{2-} diagram for the Co/$NaNO_3$ (melt) at 600°K. From reference [3].
1. $CoO+2e = Co+O^{2-}$
2. $Co_3O_4+2e = 3CoO+O^{2-}$
3. $1/2O_2+2e = O^{2-}$
4. $Co^{2+}+2e = Co$
5. $CoO = Co^{2+}+O^{2-}$
6. $Co_3O_4+2e = 3Co^{2+}+4O^{2-}$
7. $NO_3^-+2e = NO_2^-+O^{2-}$
8. $NO_2+1/2O_2+e = NO_3^-$

cobalt is in equilibrium with its dissolved ionic species. Thus, if cobalt is anodized in this region Co(II) ions should be formed according to:

$$Co = Co^{2+}+2e \qquad (2)$$

There should be no solid film and the metal should dissolve freely and continuously. As the potential increases further, a solid phase can be formed, partially blocking the passage of current. The lower potential metal-oxide line (line 1) may be extrapolated back to the active region where it represents the formation of a meta-stable film of a few molecular layers in thickness or even less. This first potential should be related to the first break of the E/log i curve, and corresponds to the formation of the Co/CoO system, represented by the following equilibrium:

$$Co+O^{2-} = CoO+2e \qquad (3)$$

As the potential rises the film grows slightly with the current barely increasing. Then, at a potential located at about 0·4–0·5 V above the potential assigned to equilibrium (3), a rapid increase of current is observed. This potential is always attained after anodizing the cobalt electrode at potentials higher than 0·3 V. According to the equilibrium potential-pO^{2-} diagram it should correspond to the formation of the Co_3O_4-CoO couple as given by:

$$3CoO+O^{2-} = Co_3O_4+2e \qquad (4)$$

At this stage, on increasing the anodic potential still further, soluble Co(II) species may be oxidized directly to form Co_3O_4 films

$$3Co^{2+}+4O^{2-} \rightarrow Co_3O_4+4e \qquad (5)$$

The overall processes just described explain the features of the E/I curves including also the spontaneous shift of the initial immersion potential towards a more positive stable value approaching the equilibrium potential corresponding to reaction (5). The spontaneous passivation of cobalt in the nitrate melt occurs through the following complementary reactions:

$$\left.\begin{aligned} 4[NO_3^-+2e &= NO_2^-+O^{2-}] \\ 3\,Co+4O^{2-} &= Co_3O_4+8e \end{aligned}\right\} \qquad (6)$$

Therefore, when a cobalt electrode is anodically polarized in the alkali nitrate melt, there is an initial unstable active dissolution of the metal at potentials near to the immersion potential and there are two breaks in the E/log I plots relating to passive states which have been assigned to CoO and Co_3O_4 formation. The first of these is better defined at higher temperatures. At higher anodic potentials metal dissolution through the Co_3O_4 film occurs, yielding as the final corrosion product, insoluble Co_3O_4. The returning E/I curves indicate clearly that the Co_3O_4 film is the stable one. The onset of passivity is characterized by a transition time on the E/t curve (Fig. 12) and the amount of charge involved corresponds to roughly one monolayer of oxide. During the occurrence of the periodic phenomena the amount of oxide playing a part during the passivation-depassivation cycle is of the order of 10^{-2} times the amount corresponding to a monolayer. Therefore under those circumstances, a relatively high rate of dissolution

should be approached at small localized islands on the oxide covered metal surface. From these results and particularly from the potential-time dependencies observed during the passivation-depassivation cycle, a diffusion-controlled mechanism can be postulated for both processes, although this is far from proven.

The potentiostatic I/t and the galvanostatic E/t responses are also interesting as they support the previous interpretation of the process and furthermore, throw some light on the shape of the $E/\log I$ curve observed at anodic potentials higher than that corresponding to equilibrium (5). The I/t curves are characterized at short time either by a current maximum or a current plateau, which resemble potentiostatic pulses observed during film formation under either film growth rate control or ohmic resistance control respectively. At longer times the current increases regularly, approaching its steady value. This corresponds to an increase of the electrode area and quite likely to metal dissolution involving pitting [7]. The relaxation processes are then in reasonable qualitative agreement with the steady measurements.

The interpretation given to the electrochemical behaviour of cobalt in molten alkali nitrate eutectics appears satisfactory within the whole temperature range investigated. However, Co(II) soluble species in the melt are no longer observed at high temperatures because of the thermal decomposition of cobalt nitrate into Co_3O_4 and nitrogen oxides [8], probably due to an increase of the concentration of species such as O_2^{2-} or O_2^- in the melt on increasing temperature [9].

Acknowledgement

This work is part of the research program of the Electrochemistry Division of INIFTA, sponsored by the Universidad Nacional de La Plata, the Consejo Nacional de Investigaciones Científicas y Técnicas and the Comisión de Investigaciones Científicas de la Provincia de Buenos Aires. J. J. Podestá acted as partime Faculty member of the Department of Engineering Chemistry, Universidad Nacional de La Plata.

References

[1] A. J. Arvía, J. J. Podestá and R. C. V. Piatti, *Electrochim. Acta*, **17** (1972) 33.
[2] A. J. Arvía, R. C. V. Piatti and J. J. Podestá, *Electrochim. Acta*, **17** (1972) 901.
[3] S. L. Marchiano and A. J. Arvía, *Anal. Soc. Cient. Arg.*, **192** (1971) 263.
[4] S. L. Marchiano and A. J. Arvía, *Electrochim. Acta*, **17** (1972) 861.
[5] D. M. Gruen, *J. Inorg. Nucl. Chem.*, **4** (1957) 74.
[6] K. E. Johnson, *Electrochim. Acta*, **11** (1966) 129.
[7] Z. Szklarska-Smialowska and M. Janik-Czachor, *Corr. Sci.*, **11** (1971) 901.
[8] R. Kirk and D. F. Othmer, *Encyclopedia of Chemical Technology*, Vol. 4, p. 206, The Interscience Encyclopedia Inc., New York (1952).
[9] J. Jordan, W. B. McCarthy and P. G. Zambonin, *Characterization and Analysis in Molten Salts*, Ed., G. Mamantov, M. Decker, New York (1969).